Table 1 Performance comparisons

Case	Method	Eigenvalue error	Computation time, s
1	Conventional method	1.0957×10^{-8}	0.22
($n = 5$)	Proposed method	2.4345×10^{-12}	0.05
2	Conventional method	1.6473×10^{-6}	0.82
($n = 10$)	Proposed method	5.3755×10^{-11}	0.22
3	Conventional method	1.5228×10^{-4}	4.45
($n = 20$)	Proposed method	2.5324×10^{-9}	0.77
4	Conventional method	6.1205×10^{-3}	13.95
($n = 30$)	Proposed method	1.8283×10^{-9}	2.25

MATLAB™ 5.2 is used.[5] The error norm of eigenvalues is defined as follows:

$$\text{error} = \sqrt{\sum_{i=1}^{2n} \frac{\left|\lambda_i - \lambda_i^c\right|^2}{|\lambda_i|^2}} \tag{32}$$

where λ_i is the desired eigenvalue of the closed-loop system and λ_i^c is the closed-loop eigenvalue that is placed by the control system. This error comes from the truncation and roundoff errors and depends on the numerical algorithms that are adopted. For this particular example, the conventional eigenstructure assignment algorithm must solve a $2n$th-order Sylvester equation numerically, and this produces much larger errors compared to the proposed algorithm. On the other hand, the proposed algorithm solves an nth-order Sylvester equation using the analytic formulation of Eqs. (30) and (31) and thereby yields more accurate result than the conventional algorithm.

Computation time is also compared and listed in Table 1. The order of floating-point operations (FLOPS) for assigning the eigenvalues by the conventional eigenstructure assignment algorithm is $\text{Lyap}(2n) + \text{inv}(n) + \text{inv}(2n) + 6n^3$. $\text{Lyap}(2n)$ indicates the FLOPS needed for solving the Lyapunov equation for a $2n \times 2n$ matrix equation, and $\text{inv}(n)$ indicates the FLOPS needed for inverting an $n \times n$ matrix. The order of FLOPS for assigning the eigenvalues by the proposed algorithm is only $\text{eig}(n) + 2 \times \text{inv}(n) + \text{inv}(2n) + 11n^3$. Note that the conventional eigenstructure assignment algorithm utilizes the Schur decomposition to solve the resulting Lyapunov equation, and therefore, it requires substantial computation time. As shown in Table 1, the conventional eigenstructure assignment algorithm requires at least three times more computation time than the proposed algorithm and loses 4–6 significant figures as well. Therefore, the proposed algorithm is at once more efficient and more accurate than the conventional eigenstructure assignment algorithm.

Conclusions

In this Note, we propose an eigenstructure assignment algorithm for the mechanical second-order system. When the proposed algorithm is used, the second-order differential equations do not have to be transformed into a higher dimensioned first-order state space to design a controller. Because the proposed algorithm is more efficient to use to design a control system for the mechanical second-order system than the conventional eigenstructure assignment algorithm in the sense of computation time and accuracy, it is better suited for incorporation into iterative computer-aided design optimization algorithms and should find wide application.

References

[1]Sobel, K. M., and Shapiro, E. Y., "A Design Methodology for Pitch-ing Pointing Flight Control Systems," *Journal of Guidance, Control, and Dynamics*, Vol. 8. No. 2, 1985, pp. 181–187.

[2]Choi, J. W., Lee, J. G., Kim, Y., and Kang, T., "Design of an Effective Controller via Disturbance Accommodating Left Eigenstructure Assignment," *Journal of Guidance, Control, and Dynamics*, Vol. 18, No. 2, 1995, pp. 347–354.

[3]Rew, D. W., Junkins, J. L., and Juang, J.-N., "Robust Eigenstructure Assignment by a Projection Method: Applications Using Multiple Optimization Criteria," *Journal of Guidance, Control, and Dynamics*, Vol. 12. No. 3, 1989, pp. 396–403.

[4]Kim, Y., Kum, D., and Nam, C., "Simultaneous Structural/Control Optimum Design of Composite Plate with Piezoelectric Actuators," *Journal of Guidance, Control, and Dynamics*, Vol. 20. No. 6, 1997, pp. 1111–1117.

[5]*MATLAB User's Guide—Control System Toolbox*, Version 4, MathWorks, Inc., Natick, MA, Dec. 1996.

[6]Junkins, J. L., and Kim, Y., *Introduction to Dynamics and Control of Flexible Structures*, AIAA, Washington, DC, 1993, pp. 206–212.

Design Technique for a Linear System with an Amplitude-Constrained Actuator

Anhtuan D. Ngo* and Uy-Loi Ly†
University of Washington, Seattle, Washington 98195-2400

I. Introduction

ACTUATOR limitations such as amplitude and rate saturations are inherent properties of all physical systems that can cause system instability. A variety of methods has been proposed to address the stability and performance of the nonlinear systems. Global stability of a chain of integrators can be achieved with a nested saturation control signal.[1] Using linear control law, one can only hope to achieve semiglobal stability for a nullcontrollable system of order three or more.[2] A design of low and high gain (LHG) linear feedback is proposed by Lin and Saberi[3] to achieve semiglobal stability for such a nullcontrollable system. Considering both stability and H_2 performance of the sytem under saturation, one can use the positive real lemma to formulate the control law to ensure stability and achieve optimal performance.[4] The issues of rate saturation and aircraft tracking performance are considered by Pachter et al.[5] in their on-line system identification and on-line optimization methods. By ganging the control effectors so that only one compensated error signal drives the effector, Hess and Snell[6] show a different way to improve stability and tracking performance in the presence of rate saturation. An optimization-based tracking control strategy is formulated in Ref. 7 to modify nonlinearly a feasible reference control signal to avoid saturating the actuators. In this paper we extend the LHG method to include the stability robustness in our approach to address the issue of control amplitude saturation.

II. Background

Theorem 1: Consider the single-input system Σ shown in Fig. 1 with $\Delta = 1$:

$$\dot{x} = Ax + B\sigma_h(u_c), \qquad x_0 \in W_0 = \{x_0 \mid |x_0| \leq m\} \tag{1}$$

and the following assumptions:

1) The pair (A, B) is stabilizable.

2) The gain and phase perturbations are represented by $\Delta = \rho$ and $e^{j\theta}$, respectively.

3) The state feedback gain G_L is chosen such that $(A - BG_L)$ is Hurwitz.

4) Let μ^* be the smallest nonnegative scalar such that, for all $\mu^* < \mu \leq 1$, $(A - \mu BG_L)$ is Hurwitz and

$$Q_H + 2G_H^T G_H + 2(1-\mu)\left(G_H^T G_L + G_L^T G_H\right) > 0 \tag{2}$$

5) The high-gain feedback $G_H = B^T P$ is obtained from the solution P of the Lyapunov equation

$$P(A - \mu BG_L) + (A - \mu BG_L)^T P = -Q_H \tag{3}$$

Received 13 October 1998; revision received 17 March 1999; accepted for publication 23 March 1999.

*Graduate Student, Department of Aeronautics and Astronautics; ngo@aa.washington.edu.

†Associate Professor, Department of Aeronautics and Astronautics. Member AIAA.

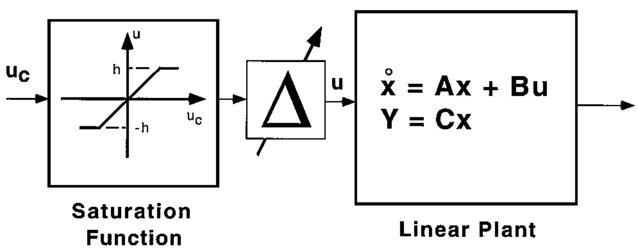

Fig. 1 Plant with uncertainty and a saturator.

with $Q_H = Q_H^T > 0$, and the parameter μ takes on a prescribed value between μ^* and 1 for robustness consideration.

Under the feedback control $u_c = -Gx$ where $G = G_L + G_H$, we have the following results:

1) The nominal closed-loop system Σ with $\Delta = 1$ will be stable for all initial conditions $x_0 \in \chi_0$ where

$$\chi_0 = \left[x_0 \text{ such that } |x_0|^2 \leq \frac{h^2 \underline{\sigma}(P)}{\bar{\sigma}\left(G_L^T G_L\right)\bar{\sigma}(P)} \right] \tag{4}$$

2) With the preceding χ_0, the closed-loop system Σ will remain stable [Eq. (1)]. For all gain perturbations $\Delta = \rho$ where $\mu \leq \rho \leq 2 - \mu$ and Eq. (2). For all phase perturbations $\Delta = e^{j\theta}$ where $-\bar{\theta} \leq \theta \leq \bar{\theta}$ and $\bar{\theta} = |\cos^{-1}(\mu)|$.

Proof: 1) Consider the Lyapunov function $V = x^T P x$. When $|u_c| < h$, from Eq. (3) we have

$$\dot{V} = -x^T\left[Q_H + 2G_H^T G_H + (1-\mu)\left(G_H^T G_L + G_L^T G_H\right)\right]x < 0$$

because of Eq. (2).

When $|u_c| \geq h$, from Eq. (3) we have

$$\dot{V} = -x^T Q_H x + 2x^T PB[\sigma_h(-G_L x - G_H x) + \mu G_L x]$$

Assume that $|G_L x| \leq h$, and we will later show that this is indeed the case for the specified χ_0. Thus, when $(-G_L x - G_H x) \geq h$ and $|G_L x| \leq h$, we have $(-G_L x - G_H x) \geq h \Rightarrow G_H x = B^T P x \leq 0$, and $(-G_L x - G_H x) \geq h \Rightarrow \sigma_h(-G_L x - G_H x) + \mu G_L x = h + \mu G_L x \geq 0$; thus $\dot{V} < 0$. The same result holds for the case when $(-G_L x - G_H x) \leq -h$.

We now show that, for the specified set of initial conditions χ_0, $|G_L x(t)| \leq h$ is indeed satisfied. Using χ_0 as defined in Eq. (4), we have

$$|G_L x_0|^2 \leq \bar{\sigma}\left(G_L^T G_L\right)\frac{h^2 \underline{\sigma}(P)}{\bar{\sigma}\left(G_L^T G_L\right)\bar{\sigma}(P)} \leq h^2$$

Because $|G_L x_0| \leq h$, we have $\dot{V}(0) < 0$. Let $V(0) = x(0)^T P x(0) \leq \bar{\sigma}(P)|x_0|^2 = \bar{V}$, and consider the time interval $0 \leq t \leq \tau_1$ during which $\dot{V}(t) < 0$. During this time interval, $V(t) = x^T(t)Px(t) < \bar{V}$. We note that $\underline{\sigma}(P)|x(t)|^2 \leq V(t)$; thus $|x(t)|^2 < \bar{V}/\underline{\sigma}(P)$. During the same time interval, we have

$$|G_L x(t)|^2 = \left|x^T(t) G_L^T G_L x(t)\right| \leq \bar{\sigma}\left(G_L^T G_L\right)|x(t)|^2$$

$$\bar{\sigma}\left(G_L^T G_L\right)|x(t)|^2 \leq \bar{\sigma}\left(G_L^T G_L\right)\frac{\bar{V}}{\underline{\sigma}(P)} = \bar{\sigma}\left(G_L^T G_L\right)\frac{\bar{\sigma}(P)|x_0|^2}{\underline{\sigma}(P)}$$

Clearly we have $|G_L x(t)| \leq h$ if

$$|x_0|^2 \leq \frac{h^2 \underline{\sigma}(P)}{\bar{\sigma}\left(G_L^T G_L\right)\bar{\sigma}(P)}$$

The same argument can also be made when we consider the next time interval for $\tau_1 \leq t \leq \tau_2$ during which $|G_L x(\tau_1)| \leq h$ and $\dot{V}(\tau_1) < 0$. Hence, $|G_L x(t)| \leq h$ for all $t \geq 0$.

2) Next, we will prove the robustness results. The closed-loop system is the one in Eq. (1) with B replaced by ρB. When $|-G_L x - G_H x| < h$, we have

$$\dot{V} = -x^T\left[Q_H + 2\rho G_H^T G_H + (\rho - \mu)\left(G_H^T G_L + G_L^T G_H\right)\right]x \tag{5}$$

With $\rho = \mu$ or $\rho = 2 - \mu$, obviously $\dot{V}$ is positive because of Eq. (2). Moreover, Eq. (5) is linear in ρ, and thus it will be positive for all $\mu \leq \rho \leq 2 - \mu$.

When $|-G_L x - G_H x| \geq h$, we have

$$\dot{V} = -x^T Q_H x + 2x^T PB[\rho\sigma_h(-G_L x - G_H x) + \mu G_L x] \tag{6}$$

Thus $\rho h + \mu G_L x \geq 0$ when $\rho \geq \max_{t \geq 0}[|G_L x(t)|/h]\mu$. Therefore, $\dot{V} < 0$ when $\rho \geq \mu$. The same result for ρ holds when we consider the case when $(-G_L x - G_H x) \leq -h$. Following the same arguments in 1), one can show that $|G_L x(t)| \leq h$ for the specified initial condition set χ_0. To show the phase margin, consider the Lyapunov function $\tilde{V}(x) = Re(x^T P x)$ and follow the same reasoning as in 1). The same semiglobal result for a chain of integrators shown in Ref. 3 can also be derived from the expression for χ_0.

III. Design Problem and Design Algorithm

Consider the single-input system shown in Fig. 1, where $A \in R^{n \times n}$, $B \in R^{n \times 1}$, $C \in R^{1 \times n}$, h is the actuator saturation level, W_0 is a finite set of initial conditions, and $\bar{\rho}$ and $\bar{\theta}$ are the gain and phase margins, respectively. The pair (A, B) is stabilizable. The problem is to design a control law G such that 1) the system Σ is stabilized for all $x(0)$ such that $|x(0)| \leq m$; 2) for $\Delta = \rho$ the system remains stable for $\bar{\rho} \leq \rho \leq 2 - \bar{\rho}$; and 3) for $\Delta = e^{j\theta}$ the system remains stable for $-\bar{\theta} \leq \theta \leq \bar{\theta}$.

The design algorithm involves interrelated design steps:

1) Select a scalar K such that $0 < K \leq 1$.

2) Design a G_L such that $(A - \mu B G_L)$ is Hurwitz for a chosen $\mu^* < \mu \leq 1$.

3) Verify that $h^2/\bar{\sigma}(G_L^T G_L) \geq m^2/K$ and $\mu \leq \min(\bar{\rho}, |\cos(\bar{\theta})|)$. If not, design a different G_L.

4) Select a $Q_H = Q_H^T > 0$ and solve for P in Eq. (3).

5) Check that Eq. (2) and $\underline{\sigma}(P)/\bar{\sigma}(P) \geq K$ are satisified. If not, find another P through Q_H.

6) Form the final control law $G = G_L + G_H$ where $G_H = B^T P$.

The region of initial conditions in which $|G_L x(t)| \leq h$ is $W_L = [x_0 \mid |x_0|^2 \leq h^2/\bar{\sigma}(G_L^T G_L)]$. This region W_L is scaled down by a factor of $\underline{\sigma}(P)/\bar{\sigma}(P)$ when the high gain G_H is added to the low gain G_L. Anticipating this, W_L is increased by a factor $1/K$ in step 2, while forcing $\underline{\sigma}(P)/\bar{\sigma}(P) > K$ is carried out in step 3. Illustrative examples are shown in the next section.

A. Example 1: Stable System

We apply the proposed design procedure to the design of a stability augmentation system for the longitudinal model of a Boeing 767 at the flight condition of 35,000-ft altitude, 0.80 Mach, 0.18 MAC. The linear model in the form of Eq. (1) is

$$x = [V(t)\ (\text{ft/s}) \quad \alpha(t)\ (\text{deg}) \quad q(t)\ (\text{deg/s}) \quad \theta(t)\ (\text{deg})]^T$$

$$A = \begin{bmatrix} -0.01675 & 0.11210 & 0.00028 & -0.56083 \\ -0.01640 & -0.77705 & 0.99453 & 0.00147 \\ -0.04167 & -3.65950 & -0.95443 & 0.00000 \\ 0.00000 & 0.00000 & 1.00000 & 0.00000 \end{bmatrix}$$

$$B = \begin{bmatrix} -0.02432 \\ -0.06339 \\ -3.69420 \\ 0 \end{bmatrix}$$

$u(t) = \Delta(t)$ (deg), $h = 8$ (deg), $W_0 = \{x_0 \mid |x_0| \leq 10\}$, $x_0^* = [5\ \ -5\ \ 5\ \ 5]^T \in W_0$, $\bar{\rho} = \frac{1}{2}$, $\bar{\theta} = 60$ deg. The airplane phugoid and short period modes are $(-0.0063 \pm j0.0592)$ and $(-0.8679 \pm j1.9061)$, respectively. We have the following design steps:

1) Because A is stable, the choice of $G_L = 0$, $K > 0$, and $0 < \mu < 0.5$ will satisfy step 3. With $\mu \approx 0$ the robustness margins are $0 \leq \rho \leq 2$, and $-90\ \text{deg} \leq \theta \leq 90$ deg.

2) With $Q_H = \text{diag}([4.752\ \ 10132\ \ 0.9801\ \ 32.604] \times 10^{-4})$, we obtain $G = G_H = [0.0167\ \ 0.0950\ \ -0.5058\ \ -1.4461]$.

3) The basin of attraction $\chi_0 \in R^4$ because $\bar{\sigma}(G_L^T G_L) = 0$. Clearly, W_0 is a subset of χ_0.

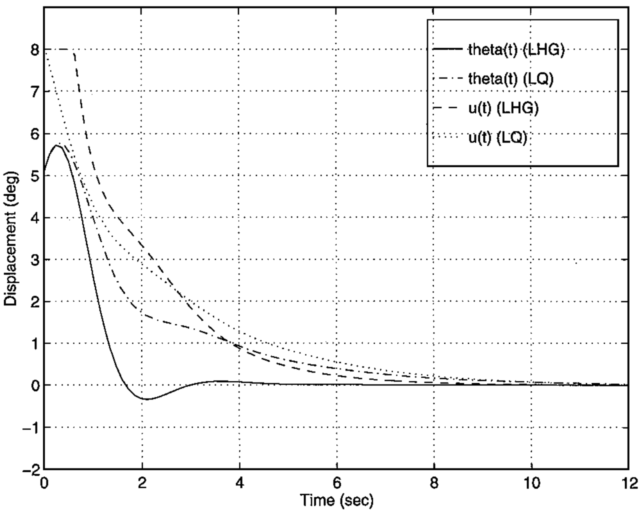

Fig. 2 Pitch-angle $\theta(t)$ response ($x_0 = x_0^*$).

The closed-loop poles are (-0.0221, -0.6833, $-1.4255 \pm j1.8741$). Although the choice of $G_L = 0$ allows us to satisfy the design requirements easily, it may not be a good design choice in terms of overall closed-loop system poles. In fact, one can see that a nonzero G_L will result in closed-loop poles located further in the left-hand side of the complex plane (see Ref. 8). In choosing Q_H we seek to minimize the performance index

$$J = \int_0^\infty \theta^2(t)\,\mathrm{d}t$$

for the particular initial condition x_0^* using a genetic algorithm (see Ref. 9). It is an open issue on how x_0^* is chosen. x_0^* can be chosen to represent the most likely encountered condition in W_0. For comparison we have also designed a linear quadratic (LQ) control law G_{LQ} that fully uses the allowed control limit $h = 8$ (deg) without experiencing saturation. The closed-loop system $\theta(t)$ and $u(t)$ responses with the LHG and LQ controllers for $x_0 = x_0^*$ can be seen in Fig. 2. Poles of the closed-loop system with the LQ feedback are (-0.0253, -0.2283, $-0.9480 \pm j1.9517$). From Fig. 2 we see that, as a result of optimizing the preceding J, the pitch angle returns to its equilibrium much faster under the LHG feedback than under the LQ design with a small undershoot. In some applications, however, a slow response with no undershoot is more desirable, making the LQ design preferable. Although the actuator rate is not considered in the design, Fig. 2 shows that the control rate is not high enough to exceed its rate limit.

B. Example 2: Unstable System

The design problem becomes more challenging when we try to apply the procedure to an unstable system. Specifically, the low-gain control law G_L cannot be set to zero; thus the region of attraction cannot be infinite. The linear model (1), taken from Ref. 10, for the F-16 aircraft at 5000-ft altitude, 0.5 Mach is $x = [\alpha(t)(\text{rad}) \;\; q(t)(\text{rad/s})]^T$:

$$A = \begin{bmatrix} -0.1606 & 0.9300 \\ 0.0939 & -0.3143 \end{bmatrix}, \qquad B = \begin{bmatrix} -0.0003 \\ -0.0127 \end{bmatrix}$$

$$u(t) = \Delta(t)\,(\text{deg}), \qquad h = 5\,(\text{deg}), \qquad W_0 = (x_0 \mid |x_0| \le 0.14)$$

$$x_0^* = [0.1 \quad 0.1]^T, \qquad \bar{\rho} = 0.8, \qquad \bar{\theta} = 30\,\text{deg}$$

The open-loop poles are (0.0679, -0.5428). Our design steps are the following:

1) We choose $K = 0.16$.

2) Solving the Riccati equation $PA + A^T P - PBR^{-1}B^T P + Q = 0$ with $R = 0.01$ and $Q = C^T C$, we have $G_L = R^{-1}B^T P = [-8.5389 \;\; -10.9840]$. From the LQ theory we know that $0.5 \le \mu \le 1$.

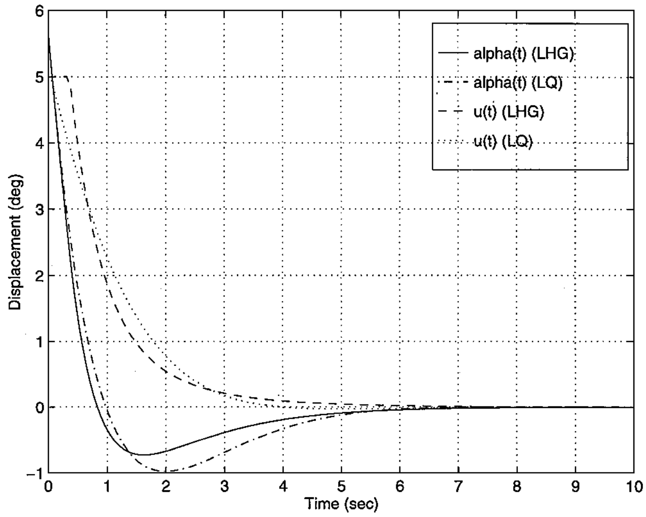

Fig. 3 Angle-of-attack $\alpha(t)$ response ($x_0 = x_0^*$).

3) We have $h^2/\bar{\sigma}(G_L^T G_L) = 0.129 \ge m^2/K = 0.122$. For the gain and phase margins required, we choose $\mu \le \min(0.8, |\cos(30\,\text{deg})|)$ or $\mu = 0.8$.

4) With $Q_H = \text{diag}([340 \;\; 1105])$, we have $G = G_L + G_H = [-26.6990 \;\; -53.6372]$.

5) Equation (2) is positive definite. Also we have $\underline{\sigma}(P)/\bar{\sigma}(P) = 0.168 \ge K = 0.160$. Thus the guaranteed gain and phase margins achieved are $0.8 \le \rho \le 1.2$, and $\cos^{-1}\mu \le \theta \le \cos^{-1}\mu$, or $-36\,\text{deg} \le \theta \le 36\,\text{deg}$.

6) From Eq. (4) the region of attraction is $\chi_0 = (x_0 \mid |x_0| \le 0.1473)$.

The closed-loop poles are (-0.7526, -1.9839). In designing G_L and Q_H we seek to speed up the airplane angle-of-attack response by minimizing the objective function

$$J = \int_0^\infty \alpha^2(x_0^*, t)\,\mathrm{d}t$$

For comparison we also have designed a linear LQ control law G_{LQ} that fully uses the allowed control limit $h = 5$ (deg) without having control saturation. The closed-loop system $\alpha(t)$ responses with the LHG and LQ controllers can be seen in Fig. 3. Figure 3 shows that, with the control saturated, the airplane angle of attack settles down to its equilibrium faster than that which is achieved when the control is not saturated. The control activities are not very fast, causing it to exceed its rate limitation.

IV. Conclusion

In this paper we have proposed a design approach to stabilize a linear system having a magnitude-constrained actuator over a set of initial conditions. In addition, system performance and robustness are also considered during the design process. The method consists of designing a nonsaturating, stabilizing, low-gain feedback that is later augmented with a high-gain feedback. The final low- and high-gain control law is free to saturate over a defined basin of attraction. Moreover, a guaranteed robustness is given for the control law. This design technique offers a practical design tool to control a real physical system.

References

[1]Teel, A. R., "Feedback Stabilization: Nonlinear Solutions to Inherently Nonlinear Problems," Electronics Research Lab., Memorandum UCB/ERL M92/65, Univ. of California, Berkeley, June 1992.

[2]Sussman, H. J., and Yang, Y., "On the Stability of Multiple Integrators by Means of Bounded Feedback Controls," Rutgers Center for Systems and Controls, Rept. SYCON-91-01, New Brunswick, NJ, Feb. 1991.

[3]Lin, Z., and Saberi, A., "A Semi-Global Low and High Gain Design Technique for Linear Systems with Input Saturation—Stabilization and Disturbance Rejection," *International Journal of Robust and Nonlinear Control*, Vol. 5, No. 5, 1995, pp. 381–398.

[4]Tyan, F., and Bernstein, D. S., "Dynamic Output Feedback Compensation for Linear Systems with Independent Amplitude and Rate Saturations,"

International Journal of Controls, Vol. 67, No. 1, 1997, pp. 89–116.

[5]Pachter, M., Chandler, P. R., and Mears, M., "Reconfigurable Flight Control with Saturation," *Journal of Guidance, Control, and Dynamics*, Vol. 18, No. 5, 1995, pp. 1016–1023.

[6]Hess, R. A., and Snell, S. A., "Flight Control Design with Rate Saturating Actuators," *Journal of Guidance, Control, and Dynamics*, Vol. 19, No. 1, 1996, pp. 38–46.

[7]Miller, R. B., and Pachter, M., "Maneuvering Flight Control with Actuator Constraints," *Journal of Guidance, Control, and Dynamics*, Vol. 20, No. 4, 1997, pp. 729–734.

[8]Ngo, A. D., "Robust Control Design for Systems with Amplitude-Constrained Actuator," Ph.D. Dissertation, Dept. of Aeronautics and Astronautics, Univ. of Washington, Seattle, WA, June 1999.

[9]Price, K., and Storn, R., "Differential Evolution," *Dr. Dobb's Journal*, Vol. 22, No. 4, 1997, pp. 18–22.

[10]Buffington, J. M., "Control Design and Analysis for Systems with Redundant Limited Controls," Ph.D. Dissertation, Dept. of Control Science and Dynamical Systems, Univ. of Minnesota, Minneapolis, MN, March, 1996.

Simple Approach to East–West Station Keeping of Geosynchronous Spacecraft

T. S. No*

Chonbuk National University, Chonju 560-756, Republic of Korea

Introduction

THE operation of geosynchronous (GEO) spacecrafts requires more precise and robust control of longitude drift because of the increase in the number of spacecrafts within the GEO orbit. As a result, the deadband of the station-keeping box for some GEO spacecrafts falls below ± 0.05 deg or less. A traditional approach to East–West (E/W) station keeping was that, at the time of crossing the deadband limit, the sign and the magnitude of the rate of mean longitude drift are restored to the predetermined values, and the magnitude and the direction of eccentricity vector are adjusted.[1–4] This idea assumes that the long-term trend in orbit evolution that is due to the perturbations is fully predictable. However, the effects of perturbations such as luni–solar attraction and solar radiation pressure vary slightly from cycle to cycle and any maneuver error will propagate to the next cycle. Therefore enough margin should be reserved to ensure that the spacecraft longitude is maintained within the deadband, even in the presence of modeling uncertainty and maneuver execution errors.

In this Note, a simple variation of traditional E/W station keeping is proposed in which the predicted drift in mean longitude and eccentricity vector at the next maneuver time is used to find the target orbit for the current maneuver planning. The results of nonlinear simulation are presented to show that the spacecraft longitude is well maintained during the free-drift period.

Linearized Equations of Orbital Motions

Since the actual orbit of GEO spacecrafts is maintained near the geostationary orbit, its evolution may be described with the following set of station-keeping elements:

$$\Delta\lambda = \lambda - \lambda_s \tag{1}$$

$$\dot{\lambda} = \frac{\mathrm{d}M}{\mathrm{d}t} - \omega_e \tag{2}$$

$$e_x = e\cos(\Omega + \omega), \qquad e_y = e\sin(\Omega + \omega) \tag{3}$$

Received 12 November 1998; revision received 27 January 1999; accepted for publication 25 February 1999.

*Assistant Professor, Department of Aerospace Engineering. Member AIAA.

where $\Delta\lambda$ denotes the longitude deviation from the nominal longitude λ_s, $\dot{\lambda}$ is the drift rate with respect to the Earth's rotation rate ω_e, and $\boldsymbol{e} = (e_x, e_y)^T$ is defined as an eccentricity vector. Other symbols such as e, Ω, ω, and M represent the classical Keplerian orbit elements. If Eqs. (1–3) are substituted into the Lagrange planetary equations,[5] after linearization one would get

$$\Delta\lambda(t) = [-3(\omega_e/V_{\mathrm{syn}})\Delta V](t-\tau)\Delta(t-\tau) + \Delta\lambda(t) \tag{4}$$

$$\Delta\dot{\lambda}(t) = [-3(\omega_e/V_{\mathrm{syn}})\Delta V]\Delta(t-\tau) + \Delta\dot{\lambda}(t) \tag{5}$$

$$\Delta e_x(t) = [(2/V_{\mathrm{syn}})\Delta V\cos\alpha]\Delta(t-\tau) + \Delta e_x(t) \tag{6}$$

$$\Delta e_y(t) = [(2/V_{\mathrm{syn}})\Delta V\sin\alpha]\Delta(t-\tau) + \Delta e_y(t) \tag{7}$$

where V_{syn} is the reference orbit speed, ΔV is the velocity increment that is due to the impulsive tangential thrusting, α is the sidereal angle of the spacecraft at the time τ of burn, and $\Delta(t-\tau)$ denotes the delta-Dirac function.

In Eqs. (4–7), $\Delta\lambda(t)$, $\Delta\dot{\lambda}(t)$, $\Delta e_x(t)$, and $\Delta e_y(t)$ represent the variations of station-keeping elements that are due to the natural perturbations acting on the GEO spacecrafts. One may numerically generate the time history of $\Delta\lambda(t)$, etc., by using the high-precision orbit propagator. If one considers their secular or long-term variations, analytical expressions could be found. A numerical technique may be used as it is known that the secular variations of $\Delta\lambda(t)$ can be well represented by a parabolic function and the mean eccentricity vector forms a circle with the period of 1 year.[1–4] In this Note, the following expressions for $\Delta\lambda$ and $\Delta\boldsymbol{e}(t)$ are assumed:

$$\Delta\lambda(t) = p_1^\lambda \times 1 + p_2^\lambda \times t + p_3^\lambda \times (t^2/2) \tag{8}$$

$$\Delta\boldsymbol{e}(t) = \boldsymbol{p}_1^e \times 1 + \boldsymbol{p}_2^e \times \sin(\omega_s t) + \boldsymbol{p}_3^e \times \cos(\omega_s t) \tag{9}$$

where ω_s denotes the sun's rotation rate and the coefficients $p_j^\lambda, \boldsymbol{p}_j^e$ are determined with a least-squares curve fit.

Predictive Targeting and Fuel Optimal Transfer

The classical targeting strategy for E/W station keeping is that, at the time of maneuver, the secular drift rate of mean longitude is compensated for to restore the predetermined target value and the direction and the magnitude of mean eccentricity vector are adjusted so that they maintain certain geometrical relationships with respect to the sun vector. With reference to Fig. 1, the amount of compensation for the drift rate and eccentricity vector at the time of maneuver t_{NOW} may be written as

$$\Delta\dot{\lambda} = \dot{\lambda}_T - \dot{\lambda}(t_{\mathrm{NOW}}) \tag{10}$$

$$\Delta\boldsymbol{e} = \boldsymbol{e}_T - \boldsymbol{e}(t_{\mathrm{NOW}}) \tag{11}$$

where $\dot{\lambda}_T$ and $\boldsymbol{e}_T$ are, respectively, the target drift rate and the eccentricity vector. If one is to use perigee-sun-tracking strategy for eccentricity control, the target for the eccentricity vector would be

$$\boldsymbol{e}_T = e_c \begin{bmatrix} \cos\left(\alpha_{\mathrm{NOW}}^s - \alpha_{\mathrm{EW}}\right) \\ \sin\left(\alpha_{\mathrm{NOW}}^s - \alpha_{\mathrm{EW}}\right) \end{bmatrix} \tag{12}$$

where α_{EW}^s is the sun's right ascension at t_{NOW}, and α_{EW}, the sun lag angle, e_c, the maximum allowable eccentricity, and $\dot{\lambda}_T$ are determined with consideration of the station-keeping cycle, T_{EW}, and the deadband budget allocation.[1] This approach is based on the assumption that the long-term trends in the variations of longitude and eccentricity vector drift will be identical or at least similar at each maneuver cycle. However, as the deadband limit gets narrower, the seasonal and short-term variations should be duly accounted for.

One possible remedy to the above problem is that the maneuver is executed so that the target orbit is achieved at the end of next free-drift period. In other words, as illustrated in Fig. 2, the target longitude and the eccentricity vector are set as follows: